was removed under reduced pressure and the oil was Kugelrohr distilled under vacuum to give **10**.

10a: 1.37 g (8.1 mmol, 81% yield) (bp 50–60 °C, 8 mmHg); ^{1}H NMR (300 MHz) ($CDCl_3$) δ 0.85 (s, 6 H), 0.86 (d, 6 H, J = 6.6 Hz), 0.87 (bs, 1 H), 1.71 (tsept, 1 H, J = 6.9, 6.6 Hz), 1.98 (d, 2 H, J = 7.5 Hz), 2.29 (s, 2 H), 2.35 (d, 2 H, J = 6.9 Hz), 4.99 (m, 2 H), 5.79 (ddt, 1 H, J = 9.2, 17.9, 7.5 Hz); ^{13}C NMR (75.5 MHz) ($CDCl_3$) δ 20.6, 25.5, 27.9, 34.4, 44.7, 59.1, 60.3, 116.6, 135.7; IR (neat) 3359, 3077, 3005, 2957, 2872, 2811, 1640, 1466, 1385, 1364, 1121, 995, 912 cm^{-1}. Anal. Calcd for $C_{11}H_{23}N$: C, 78.04; H, 13.69; N, 8.27. Found: C, 77.64; H, 13.87; N, 7.68.

***N*-Methyl-*N*-isobutyl-2,2-dimethylpent-4-enamine (12).** To 25 mL of dry acetonitrile were added 0.847 g (5 mmol) of **10a** and 0.710 g (5 mmol) of MeI. The solution was heated to reflux for 12.5 h and then cooled to ambient temperature. Solvent was removed under reduced pressure and the residue was washed with 10 mL of 15% aqueous NaOH and extracted with 3 × 50 mL portions of Et_2O. The organic layers were combined, dried ($MgSO_4$), filtered, and concentrated under reduced pressure. Kugelrohr distillation under vacuum gave 0.739 g (4.0 mmol, 81% yield) of **12** (bp 60–70 °C, 10 mmHg): ^{1}H NMR (300 MHz) ($CDCl_3$) δ 0.82 (s, 6 H), 0.87 (d, 6 H, J = 6.6 Hz), 1.65 (tsept, 1 H, J = 7.4, 6.6 Hz), 1.97 (d, 2 H, J = 7.4 Hz), 2.07 (s, 2 H), 2.10 (d, 2 H, J = 7.4 Hz), 2.18 (s, 3 H), 4.97 (m, 2 H), 5.81 (ddt, 1 H, J = 11.0, 18.8, 7.4 Hz); ^{13}C NMR (75.5 MHz) ($CDCl_3$) δ 20.6, 25.4, 26.8, 36.0, 44.9, 45.0, 69.5, 70.2, 116.6, 136.4; IR (neat) 3077, 2978, 2843, 2786, 1640, 1470, 1385, 1366, 1250, 1105, 1040, 993, 909, 850 cm^{-1}. Anal. Calcd for $C_{12}H_{25}N$: C, 78.62; H, 13.74; N, 7.64. Found: C, 78.55; H, 13.48; N, 7.70.

(18) In the case of the more volatile compounds **10a** and **10b**, an excess of aqueous HCl was added, and the solution was concentrated under reduced pressure. The residue was treated with 15% aqueous NaOH to a pH of 14, the amine was extracted with 3 × 50 mL portions of Et_2O, and the organic layers were dried ($MgSO_4$) prior to distillation.

MeI-Promoted Rearrangement of 8a Followed by $LiAlH_4$ Reduction. To 15 mL of 1,4-dioxane were added 1.34 g (8 mmol) of enamine **8a** and 1.14 g (8 mmol) of MeI. The solution was heated to reflux for 17 h and then cooled to 0 °C. The reaction was reduced by addition of $LiAlH_4$ (16.0 mL, 1 M in THF, 16 mmol), warming to ambient temperature, and then stirring for 2 h. The solution was then cooled to 0 °C and quenched by addition of 0.6 mL of water, 0.6 mL of 15% aqueous NaOH, and 1.8 mL of water. After being stirred for 1 h, the mixture was filtered and then treated with an excess of aqueous HCl. The solution was concentrated under reduced pressure and the residue was treated with 15% aqueous NaOH to a pH of 14. The amine products were extracted with 3 × 50 mL portions of Et_2O and the organic layer was dried ($MgSO_4$). Volatiles were removed by rotary evaporation and the oil was Kugelrohr distilled under vacuum to give 0.81 g (59% yield) of an 89:11 mixture of *N*-isobutyl-2,2-dimethylpent-4-enamine (**10a**) and *N*-methyl-*N*-isobutyl-2,2-dimethylpent-4-enamine (**12**) (bp 60–65 °C, 10 mmHg).

MeOTs-Promoted Rearrangement of 8a Followed by $LiAlH_4$ Reduction. The reaction was performed under conditions identical with those described above, using 1.49 g (8 mmol) of MeOTs. Distillation after workup gave 0.95 g (68% yield) of a 72:28 mixture of *N*-isobutyl-2,2-dimethylpent-4-enamine (**10a**) and *N*-methyl-*N*-isobutyl-2,2-dimethylpent-4-enamine (**12**) (bp 60–65 °C, 10 mmHg).

Acknowledgment. We are grateful to Michigan State University for support of this research. The NMR data were obtained on instrumentation purchased in part with funds from NIH grant 1-S10-RR04750-01 and from NSF grant CHE-88-00770.

Supplementary Material Available: Experimental procedures and physical data for the series of compounds **b–g** (5 pages). Ordering information is given on any current masthead page.

Metal-Ion Catalysis in Nucleophilic Displacement Reactions at Carbon, Phosphorus, and Sulfur Centers.† 5. Alkali-Metal Ion Catalysis and Inhibition in the Reaction of *p*-(Trifluoromethyl)phenyl Methanesulfonate with Ethoxide Ion

Marko J. Pregel and Erwin Buncel*

Department of Chemistry, Queen's University, Kingston, Ontario, Canada K7L 3N6

Received May 29, 1991

The reactions of alkali-metal ethoxides with *p*-(trifluoromethyl)phenyl methanesulfonate (1) in anhydrous ethanol at 25 °C, yielding *p*-(trifluoromethyl)phenolate ion and ethyl methanesulfonate, have been investigated in order to reveal the effects of alkali-metal ions on reaction rates. Kinetic spectrophotometric studies of the nucleophilic displacement reaction of 1 with alkali-metal ethoxides in the absence and presence of complexing agents showed that the observed rate constants increase in the order LiOEt < EtO^- < NaOEt < CsOEt < KOEt. Thus, Li^+ inhibits the reaction of ethoxide ion, while the other alkali-metal ions all act as catalysts. The kinetic data are analyzed in terms of parallel reactions of free ethoxide ion and alkali-metal ethoxide ion pairs, and rate constants for the reactions of these species are calculated. Association constants governing the interaction of the various metal ions with the transition state for the reaction of ethoxide ion with 1 are derived from the kinetic data and compared to association constants for interaction of metal ions with ethoxide ion in the ground state. The trend in the sizes of the association constants for the methanesulfonate transition state, Li^+ < Na^+ < K^+ < Cs^+, is believed to arise from ion pairing of the transition state with solvated metal ions. A similar ordering is observed for the transition state in the reaction of *p*-nitrophenyl benzenesulfonate (2) with alkali metal ethoxides, while an inverted ordering is seen for the transition state for the reaction of ethoxides with *p*-nitrophenyl diphenylphosphinate (3). These results are interpreted in terms of the extent of charge delocalization in the transition states and its effect on interactions with bare or solvated metal ions.

Introduction

As part of a series of systematic studies of the mechanisms of reaction of carbon-, phosphorus-, and sulfur-based esters, and the effects of alkali-metal ions on these reactions, we report here on alkali-metal ion catalysis and inhibition in the reaction of ethoxide ion with *p*-(trifluoromethyl)phenyl methanesulfonate (1) in anhydrous ethanol at 25 °C. The purpose of these studies has been to explain the interesting and unusual finding that some alkali-metal ions catalyze the reactions of ethoxide ion with 1 and with *p*-nitrophenyl benzenesulfonate (2), while

†This paper is an extension of our series on Bond Scission in Sulfur Compounds. For previous papers in this series, see ref 1.

0022-3263/91/1956-5583$02.50/0

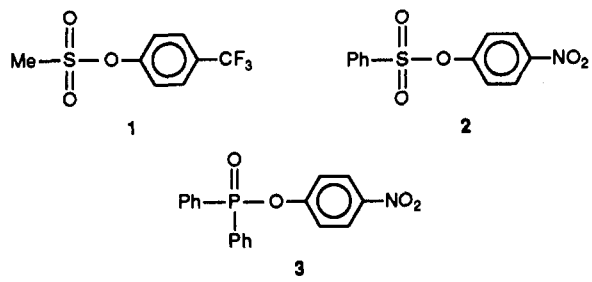

others inhibit the reactions. In contrast, all alkali-metal ions studied catalyze the reaction of ethoxide ion with *p*-nitrophenyl diphenylphosphinate (3). A detailed explanation of this phenomenon may have implications for a better understanding of the effects of alkali-metal ions in biological systems, in which discrimination among alkali-metal ions is also observed.[2]

Previous reports demonstrated alkali-metal ion catalysis (Na^+, K^+, and Cs^+) and inhibition (Li^+) in the nucleophilic displacement reaction of ethoxide with *p*-nitrophenyl benzenesulfonate (2),[1e,g] as well as alkali-metal ion catalysis in the nucleophilic displacement reaction of *p*-nitrophenyl diphenylphosphinate (3) with ethoxide.[1d] Further studies characterized the nucleophilic substitution reaction of aryl benzenesulfonate and aryl diphenylphosphinate esters with ethoxide as being associative, with well-advanced bond formation to the nucleophile but little leaving-group bond breakage in the transition state.[1h,j]

In order to investigate a possible difference in mechanism between aryl benzenesulfonate and aryl methanesulfonate esters, the mechanisms of reaction of *p*-nitrophenyl, *m*-nitrophenyl, and *p*-(trifluoromethyl)phenyl (1) methanesulfonates with ethoxide were investigated. It was concluded that the *p*-nitro-substituted ester reacts predominantly by an E1cb-type elimination mechanism via a sulfene intermediate, with nucleophilic substitution as a minor concurrent pathway. Conversely, the *m*-nitro-substituted ester was found to react predominantly by substitution at sulfur, with elimination as a minor pathway. The available evidence indicated that the *p*-trifluoromethyl-substituted ester reacts solely by nucleophilic substitution at sulfur.[1i]

This report presents metal-ion effects on the reaction of ethoxide ion with 1, which are compared and contrasted to metal-ion effects in the analogous reactions of 2 and 3. Our discussion focuses on metal-ion effects in the transition states of these reactions, and it is assumed that a common set of principles underlies the differing results seen in the three systems.

Results and Discussion

Kinetic Studies. Kinetic data for the reaction of *p*-(trifluoromethyl)phenyl methanesulfonate (1) with alkali-metal ethoxides in the absence and presence of crown ether and cryptand complexing agents are presented in Figure 1 and Table I. The pseudo-first-order rate constants (k_{obs}) for the reaction of ester with excess base were determined spectrophotometrically in anhydrous ethanol at 25 °C. Following our previous treatment of the data for reactions of alkali-metal ethoxides with esters,[1d,g,h] the more or less curved plots of k_{obs} vs $[MOEt]_o$ are interpreted

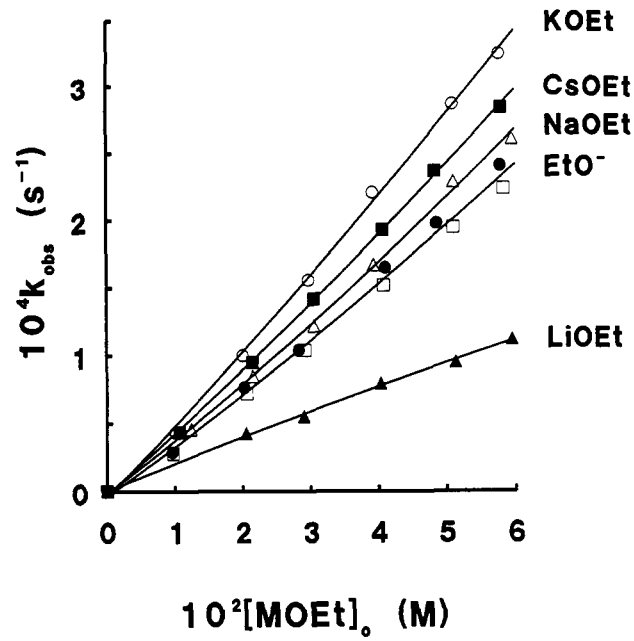

Figure 1. Kinetic data for the reaction of *p*-(trifluoromethyl)-phenyl methanesulfonate (1) with LiOEt (▲), NaOEt (△), KOEt (○), and CsOEt (■) as well as KOEt in the presence of excess 18-crown-6 (□) and KOEt in the presence of excess cryptand 222 (●).

Table I. Kinetic Data for the Reaction of 1 with Alkali-Metal Ethoxides in EtOH at 25 °C

	10^2-$[MOEt]_o$ (M)	10^4k_{obs} (s^{-1})
LiOEt	2.05	0.427
	2.90	0.552
	4.03	0.792
	5.13	0.952
	5.95	1.12
NaOEt	1.24	0.459
	2.15	0.846
	3.05	1.22
	3.93	1.67
	5.10	2.29
	5.95	2.61
KOEt	1.01	0.433
	2.00	1.00
	2.97	1.56
	3.92	2.21
	5.10	2.87
	5.78	3.25
CsOEt	1.07	0.435
	2.15	0.949
	3.05	1.42
	4.07	1.93
	4.83	2.37
	5.80	2.84
KOEt + 18C6; [18C6]/[KOEt] = 1.48	0.972	0.279
	2.06	0.718
	2.92	1.04
	4.08	1.52
	5.10	1.95
	5.83	2.24
KOEt + 222; [222]/[KOEt] = 1.46	0.962	0.289
	2.02	0.763
	2.83	1.04
	4.10	1.65
	4.86	1.98
	5.78	2.41

(1) (a) Buncel, E.; Wilson, H.; Chuaqui, C. *J. Am. Chem. Soc.* **1982**, *104*, 4896. (b) Buncel, E.; Chuaqui, C.; Wilson, H. *J. Org. Chem.* **1980**, *45*, 2825. (c) Buncel, E.; Dunn, E. J.; Bannard, R. A. B.; Purdon, J. G. *J. Chem. Soc., Chem. Commun.* **1984**, 162. (d) Dunn, E. J.; Buncel, E. *Can. J. Chem.* **1989**, *67*, 1440. (e) Pregel, M. J.; Buncel, E. *J. Chem. Soc., Chem. Commun.* **1989**, 1566. (f) Dunn, E. J.; Moir, R. Y.; Buncel, E.; Purdon, J. G.; Bannard, R. A. B. *Can. J. Chem.* **1990**, *68*, 1837. (g) Pregel, M. J.; Dunn, E. J.; Buncel, E. *Can. J. Chem.* **1990**, *68*, 1846. (h) Pregel, M. J.; Buncel, E. *J. Am. Chem. Soc.*, **1991**, *113*, 3545. (i) Pregel, M. J.; Buncel, E. *J. Chem. Soc., Perkin Trans. 2* **1991**, 307. (j) Dunn, E. J.; Buncel, E. Unpublished results.

(2) Suelter, C. H. In *Metal Ions in Biological Systems*; Sigel, H., Ed.; Marcel Dekker: New York, 1976; Vol. 3, Chapter 7.

Table II. Free-Ion and Ion-Pair Rate Constants for the Reaction of Various Ethoxide Species with 1-3 in EtOH at 25 °C

base	k (M^{-1} s^{-1}) 1	2[1g]	3[1d]
LiOEt	0.0015	0.0180	24.0
NaOEt	0.0055	0.080	11.6
KOEt	0.0074	0.137	4.84
CsOEt	0.0060	0.097	1.89
EtO^-	0.0030	0.0287	0.980

as arising from parallel reactions of free ethoxide ion and alkali-metal ethoxide ion pairs (eq 1). An ion-pair asso-

$$M^+ + EtO^- + PhSO_2OAr \xrightarrow{k_{EtO^-}} \text{products}$$
$$K_a \Big\| \Big\uparrow \qquad (1)$$
$$MOEt + PhSO_2OAr \xrightarrow{k_{MOEt}} \text{products}$$

ciation constant, K_a, governs the equilibrium between free ions and ion pairs (eq 2), both of which may react with the ester. The observed rate constant is a sum of contributions from the free-ion and ion-pair pathways (eq 3). Since K_a

$$M^+ + EtO^- \rightleftarrows MOEt \qquad K_a = \frac{[MOEt]}{[M^+][EtO^-]} \qquad (2)$$

$$k_{obs} = k_{EtO^-}[EtO^-] + k_{MOEt}[MOEt] \qquad (3)$$

>1 M^{-1} for all alkali-metal ethoxides, the ratio of ion pairs to free ions increases as the total base concentration increases, and the balance between the free-ion and ion-pair pathways changes in favor of the ion-pair pathway. Since free ions and ion pairs differ in reactivity, this results in curved plots of observed rate constant vs total base concentration. Upward curvature is seen when $k_{MOEt} > k_{EtO^-}$ and downward curvature is seen when $k_{MOEt} < k_{EtO^-}$. K_a values for alkali-metal ethoxides in anhydrous ethanol at 25 °C have been determined,[3] so equilibrium concentrations of free ions and ion pairs can be calculated since the total base concentration is known and $[M^+] = [EtO^-]$ at equilibrium. Consequently, variation of the observed pseudo-first-order rate constant with the total base concentration may be used to determine second-order rate constants for free ethoxide and metal-ethoxide ion pairs using eq 4.

$$\frac{k_{obs}}{[EtO^-]} = k_{EtO^-} + k_{MOEt}K_a[EtO^-] \qquad (4)$$

The second-order rate constants for the reaction of 1 with LiOEt, NaOEt, KOEt, and CsOEt are presented in Table II. The second-order rate constant for the reaction of free ethoxide ion, calculated from data on KOEt + 18C6 (the slope of a plot of k_{obs} vs $[MOEt]_o$ extrapolated to zero base concentration], is also found in Table II. As expected, KOEt, CsOEt, and NaOEt ion pairs are more reactive than free ethoxide ion, consistent with the observed ordering of curves of k_{obs} vs $[MOEt]_o$ and the upward curvature of these plots. Similarly, the LiOEt ion pair is seen to be less reactive than ethoxide ion.

An alternate interpretation of the data is that metal-ion effects arise through complexation of the ester prior to its reaction with ethoxide ion.[4,5] However, the ion-pair

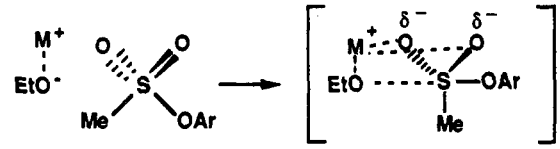

Figure 2. Representation of metal-ion catalysis via attack of an alkali-metal ethoxide ion pair on an aryl methanesulfonate ester.

Scheme I

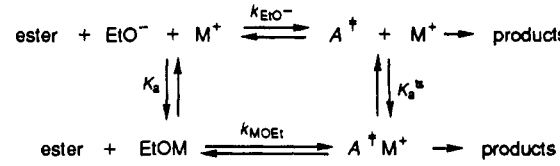

Table III. Association Constants for the Interaction of Various Metal Ions with the Transition States (K_a^{ts}) and Ground State (EtO^-, K_a) for the Reaction of EtO^- with 1-3 (K_a Values Are from ref 3). All Values Are in Units of M^{-1}

	K_a	K_a^{ts} (1)	K_a^{ts} (2)	K_a^{ts} (3)
Li^+	212	106	133	5192
Na^+	102	187	284	1207
K^+	90	222	430	445
Cs^+	121	242	409	233

mechanism is preferred for the following reasons. First, there have been no reports suggesting that alkali-metal ions complex sulfonate esters in alcoholic media to an appreciable extent. Second, previous studies of reactions of alkali-metal ethoxides with alkyl halides[6,7] and carboxylate esters[8] in ethanol have provided evidence for reactive ion pairs. Third, when the preassociation mechanism was assumed for ester 2, the kinetic model required the complexed ester to have an unrealistically high reactivity.[1g]

The reaction of alkali-metal ethoxide ion pairs with sulfonate esters is believed to occur as shown in Figure 2. Thus, attack of an ion pair on the ester is an example of "push-pull" catalysis with simultaneous charge donation (by ethoxide ion to the electropositive sulfonate sulfur) and charge removal (by the metal ion from the electron-rich sulfonyl oxygens). Stabilization of the transition state by metal ions is believed to occur by chelation to the negatively charged sulfonyl oxygens.

Dissection of Metal-Ion Effects into Ground-State and Transition-State Contributions. For the reaction of alkali-metal ethoxides with *p*-(trifluoromethyl)phenyl methanesulfonate (1), the results of previous studies are consistent with a nucleophilic substitution mechanism.[1i] The kinetic studies reported here have shown that Na^+, K^+, and Cs^+ cause rate accelerations, while Li^+ causes a rate retardation. The observed order of reactivity of alkali-metal ethoxides with 1 (Table I) is identical with the reactivity order for the aryl benzenesulfonate 2 (LiOEt < EtO^- < NaOEt < CsOEt < KOEt),[1g] but quite different from that of the aryl diphenylphosphinate 3 (CsOEt < KOEt < NaOEt < LiOEt (Table I)).[1d]

All three esters are believed to react with ethoxide ion by an associative mechanism having a transition state in

(3) Barthel, J.; Justice, J.-C.; Wachter, R. *Z. Phys. Chemie Neue Folge* **1973**, *84*, 100.
(4) Cooperman, B. The Role of Divalent Metal Ions in Phosphoryl and Nucleotidyl Transfer. In *Metal Ions in Biological Systems*; Sigel, H., Ed.; Marcel Dekker: New York, 1974; Vol. 5.
(5) Mildvan, A. C.; Grisham, C. M. The Role of Divalent Cations in the Mechanism of Enzyme Catalyzed Phosphoryl and Nucleotidyl Transfer Reactions. In *Structure and Bonding*; Dunitz, J. D., Hemmerich, P., Holm, R. H., Ibers, J. A., Jorgensen, C. K., Nielands, J. B., Reiner, D., Williams, R. J. P., Eds.; Springer Verlag: New York, 1974; Vol. 20.
(6) Cayzergues, P.; Georgoulis, C.; Mathieu, G. *J. Chim. Phys.* **1987**, *84*, 55.
(7) Papoutsis, A.; Papanastasiou, G.; Jannakoudakis, D.; Georgoulis, C. *J. Chim. Phys.* **1985**, *82*, 913.
(8) Barthel, J.; Bader, G.; Raach-Lenz, M. *Z. Phys. Chemie* **1976**, *103*, 135.

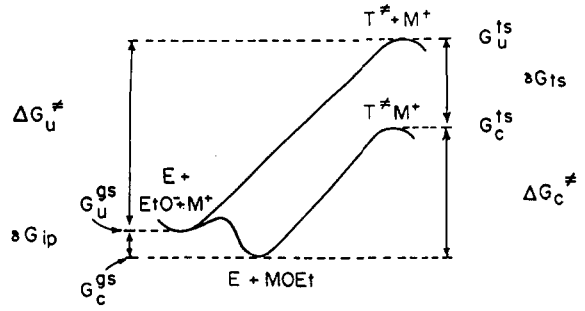

Figure 3. Free energies (G) involved in the ground state (ip) and transition state (ts) of the uncatalyzed (u) and metal ion catalyzed (c) reaction of an ester (E) with ethoxide ion (EtO^-).

which nucleophilic attack is well-advanced but leaving-group bond breakage is minimal. Metal-ion effects may be discussed in terms of interactions of metal ions in the ground state and transition state. Ground-state interactions, i.e., association of alkali-metal ions with ethoxide ion, are identical in all three systems, so the differing metal-ion effects must arise from differences in metal-ion interactions in the transition states. The determination of the magnitudes of these transition-state interactions from the kinetic data is described below.

In order to differentiate the ground-state and transition-state effects that contribute to the observed rate constants, the parallel free-ion and ion-pair pathways may be written as a set of equilibria among the various reactants (the ester, free and ion-paired ethoxides) and transition states (Scheme I). This allows the calculation of a virtual association constant for the interaction of a metal ion with the transition state of the reaction of ethoxide ion with the ester (K_a^{ts}) using eq 5.[9] K_a^{ts} values are presented and

$$K_a^{ts} = \frac{k_{MOEt} K_a}{k_{EtO^-}} \tag{5}$$

compared to their respective K_a values in Table III. For **1** it is seen that $K_a^{ts} > K_a$ for Na^+, K^+, and Cs^+: these metal ions stabilize the transition state of the reaction more than they stabilize ethoxide ion in the ground state and act as catalysts. Conversely, K_a^{ts} (Li^+) < K_a (LiOEt): lithium ion stabilizes ethoxide ion in the ground state more than it stabilizes the transition state and acts as an inhibitor (cf. ref 10).

Metal-ion stabilization of the ground and transition states is shown in the free energy diagram of Figure 3.[11] $\Delta G_u^{\ddagger}$ and $\Delta G_c^{\ddagger}$ represent the free energies of activation of the uncatalyzed and catalyzed reactions, respectively, while δG_{ip} and δG_{ts} refer to the free energies for association of a metal ion to ethoxide ion and to the transition state, respectively. The net catalytic effect of the metal ion is given by $\Delta G_{cat.}$, the difference in free energies of activation between the catalyzed and uncatalyzed reactions.

$$-\delta G_{ip} + \Delta G_u^{\ddagger} = \Delta G_c^{\ddagger} - \delta G_{ts} \tag{6}$$

$$\Delta G_{cat.} = \Delta G_c^{\ddagger} - \Delta G_u^{\ddagger} = \delta G_{ts} - \delta G_{ip} \tag{7}$$

The free energy diagram of Figure 3 shows that δG_{ts} measures the stabilization of the transition state by the metal ion. This represents the maximum catalytic potential of the metal ion for the reaction.[11] In contrast, δG_{ip} measures the stabilization of the ground state by the metal ion, which detracts from its catalytic effect. $\Delta G_{cat.}$ is the difference between δG_{ts} and δG_{ip} (eq 7) and is a measure of the net catalytic effect of the metal ion. Thus, $\Delta G_{cat.}$ is related to the ratio of the second-order rate constant for a particular alkali-metal ethoxide (k_{MOEt}) to the rate constant for free ethoxide ion (k_{EtO^-}) (eq 12). In terms of association constants, $\Delta G_{cat.}$ is related to the ratio of the association constant of the metal ion with the transition state (K_a^{ts}) to its association constant with the ground state (K_a).

Table IV. Free Energies of Metal-Ion Stabilization of Ethoxide Ion (δG_{ip}) and of the Transition States (δG_{ts}) for the Reaction of Ethoxide with 1–3 as well as Overall Catalytic Effect of Each Metal Ion ($\Delta G_{cat.}$) in the Reaction of 1 (kJ mol^{-1})

	δG_{ip}	δG_{ts} (1)	δG_{ts} (2)	δG_{ts} (3)	$\Delta G_{cat.}$ (1)
Li^+	−13.3	−11.6	−12.1	−21.2	+1.7
Na^+	−11.5	−13.0	−14.0	−17.6	−1.5
K^+	−11.2	−13.4	−15.0	−15.1	−2.2
Cs^+	−11.9	−13.6	−14.9	−13.5	−1.7

$$\delta G_{ip} = -RT \ln K_a \tag{8}$$

$$\delta G_{ts} = -RT \ln K_a^{ts} \tag{9}$$

$$\Delta G_u^{\ddagger} = -RT \ln k_{EtO^-} + A \tag{10}$$

$$\Delta G_c^{\ddagger} = -RT \ln k_{MOEt} + A \qquad A = \text{constant} \tag{11}$$

$$\Delta G_{cat.} = -RT \ln (k_{MOEt}/k_{EtO^-}) = -RT \ln (K_a^{ts}/K_a) \tag{12}$$

The various free energies in the reaction of **1** are summarized in Table IV and compared to the corresponding values for *p*-nitrophenyl benzenesulfonate (**2**) and *p*-nitrophenyl diphenylphosphinate (**3**). For **1**, the trend in the values of $\Delta G_{cat.}$ parallels the trend in k values: maximum catalysis is seen for K^+, followed by Cs^+, Na^+, and Li^+. Potassium ion is the best catalyst because it has the strongest association with the transition state and the weakest association with the ground state. The trend in δG_{ts} values does not parallel the trend in $\Delta G_{cat.}$ values because the former refer to transition-state effects only, while the latter contain both ground-state and transition-state contributions.

The results in Table IV show that trends in δG_{ts} values for various ions are similar for **1** and **2**, but different for **3**. The ordering changes from $K^+ < Cs^+$ in **2** to $Cs^+ < K^+$ in **1**. Conversely, the ordering for **3** is exactly the opposite to that of **1**.

Differing selectivity patterns for alkali-metal ions have also been observed for ion-exchange resins and glass electrodes, and the phenomenon has been explained in terms of two competing effects:[12] (1) electrostatic interaction between the anionic group (the transition state in the present case) and its alkali-metal counterion and (2) rearrangement of solvent molecules to permit the anion and counterion to come into direct contact (solvation/desolvation). The anion and solvent may be said to compete for the metal ion.[13] Anionic groups with high electric field strengths (localized charges) win the contest and attract cations away from solvent, so the anion interacts with bare metal ions. On the basis of Coulomb's Law, the smallest cations are attracted most strongly (bare cations in this case), so the order of affinities is $Li^+ > Na^+ > K^+$

(9) Kurz, J. L. *J. Am. Chem. Soc.* **1963**, *85*, 987.
(10) (a) Buncel, E.; Wilson, H. *J. Chem. Ed.* **1980**, *9*, 629. (b) Buncel, E.; Wilson, H. *Acc. Chem. Res.* **1979**, *12*, 42.
(11) Schowen, R. L. In *Transition States of Biochemical Processes*; Gandour, R. D., Schowen, R. L., Eds.; Plenum Press: New York and London, 1978; Chapter 2.
(12) Reichenberg, D. In *Ion Exchange*; Marinsky, J. A., Ed.; Marcel-Dekker: New York, 1966; Vol. 1, Chapter 7.
(13) Rieman, W.; Walton, H. F. *Ion Exchange in Analytical Chemistry*; Pergamon Press: Oxford, 1970.
(14) Fenton, D. E. Alkali Metals and Group IIA Metals. In *Comprehensive Coordination Chemistry*; Wilkinson, G., Ed.; Pergamon Press: Oxford, 1987.

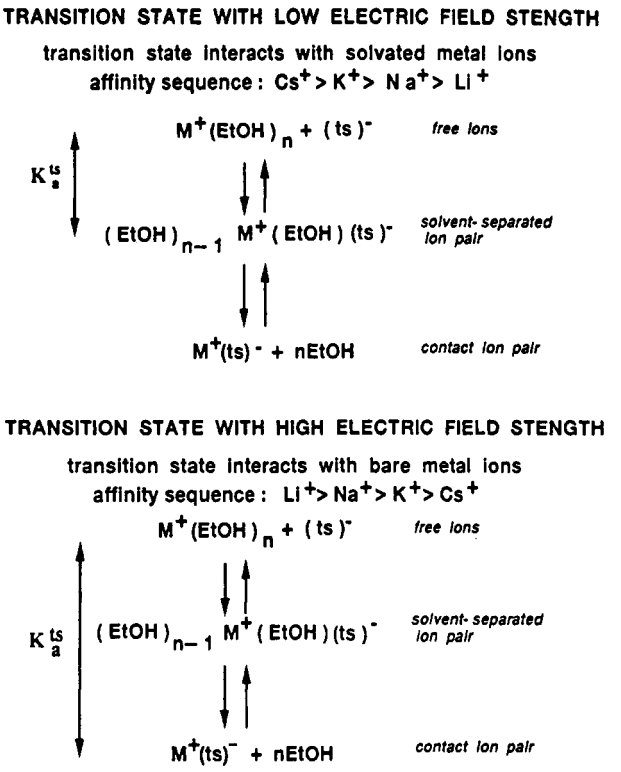

Figure 4. Representation of interactions among bare and solvated metal ions and charge-localized (high electric field strength) and charge-delocalized (low electric field strength) transition states.

> Cs^+. This ordering is found in practice for carboxylate ion-exchange resins and is consistent with the small size and high electric field strength of the carboxylate group. This ordering is also seen in δG_{ts} values for the phosphinate transition state, indicating a high electric field strength and consistent with a negative charge localized on a single oxygen.

Conversely, anionic groups with low electric field strengths lose the contest with solvent for the metal ion. The cations remain solvated, leaving the ions with the smaller *solvated* radii to be bound most strongly.[13] The affinity sequence in this case is $Cs^+ > K^+ > Na^+ > Li^+$. The sulfonate group (RSO_3^-) is believed to have a low electric field strength, and in fact, many different types of ion-exchange resins containing sulfonate groups have displayed the affinity sequence described above.[12]

The methanesulfonate transition state, which has its charge delocalized over two or more oxygens, is expected to have weak interactions with metal ions and may not be able to displace a solvent molecule from the coordination sphere of the metal ion.[12,13] Consequently, the transition state may be expected to interact with solvated metal ions, and this results in δG_{ts} values increasing in the order $Cs^+ < K^+ < Na^+ < Li^+$, due to stronger interactions between the transition state and metal ions with smaller *solvated* radii. Interactions of transition states with high and low electric field strengths with bare and solvated ions are depicted in Figure 4.

As expected when an anion interacts with solvated metal ions, there is a linear relationship between the free energy of association of the metal ion with the transition state (δG_{ts}) and the size of the solvated ion (r_{Stokes}^{corr}). A linear plot of δG_{ts} vs $1/r_{Stokes}^{corr}$ (Figure 5a) shows that for 1 the free energy of association increases linearly with the electrostatic potential of the metal ion, which is proportional to the inverse of its solvated radius. Solvated (Stokes) radii were calculated from conductivity data[3] then

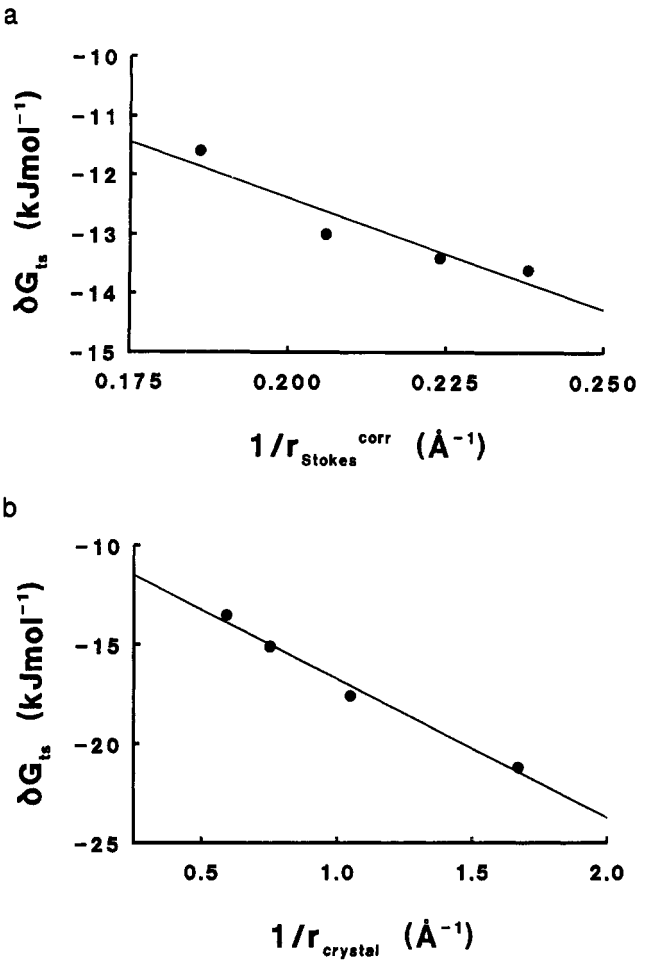

Figure 5. a: Plot of δG_{ts} vs the reciprocal of the corrected Stokes radius of the metal ion for the reaction of 1 with alkali-metal ethoxides in EtOH at 25 °C ($r = -0.942$). b: Plot of δG_{ts} vs the reciprocal of the crystal radius of the metal ion for the reaction of 3 with alkali-metal ethoxides in EtOH at 25 °C ($r = -0.993$).

corrected for underestimation of solvated radii by the Stokes equation using the method of Della Monica and Senatore.[15]

Conversely, the δG_{ts} values for the phosphinate transition state vary linearly with the inverse of the radii of the bare metal ions (r_{cryst}), consistent with the high electric field strength of this species (Figure 5b). Also consistent with our hypothesis, δG_{ts} values for the phosphinate transition state (3) are significantly greater than those of both 1 and 2. According to Coulomb's Law the strength of the transition-state metal-ion interaction should vary inversely with the radius of the metal ion. Since the bare alkali-metal ions are much smaller than solvated alkali-metal ions, it follows that δG_{ts} values should be greater when bare metal ions interact with the transition state.

From the above arguments, it follows that, as the field strength of the anion is increased, the affinity sequence will change from $Cs^+ > K^+ > Na^+ > Li^+$ (the order of solvated radii and the ordering observed for 1) to $Li^+ > Na^+ > K^+ > Cs^+$ (the order of crystal radii and the ordering observed for 3) with a number of different sequences as intermediates. The ordering of the intermediate sequences may be predicted for aqueous solutions, and they are presented in Figure 6.[12,13] It is interesting to note that selectivity sequences found for ionophore antibiotics and

(15) Della Monica, M.; Senatore, L. *J. Phys. Chem.* **1970**, *74*, 205.

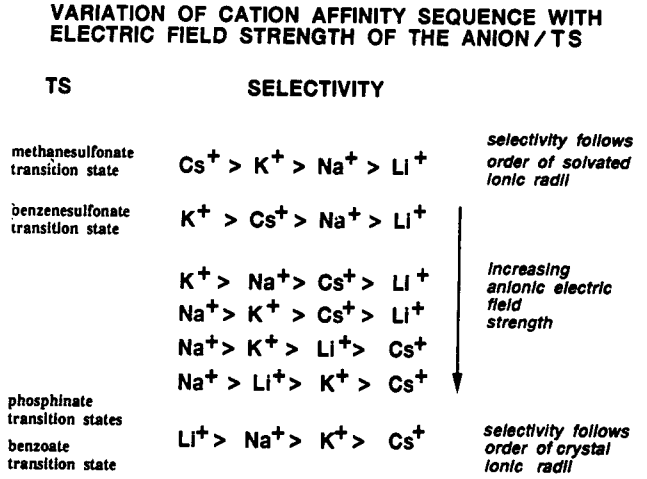

Figure 6. Variation of cation affinity sequence with electric-field strength of the anion (refs 12, 13).

crown ethers are all among those predicted by this treatment.[14] In contrast, the sequence of association constants of alkali-metal ions with ethoxide ion does not fall among the predicted sequences.

In Figure 6, as the field strength is increased, the first change is from $Cs^+ > K^+ > Na^+ > Li^+$ to $K^+ > Cs^+ > Na^+ > Li^+$ (the ordering observed for **2**), indicating that the transition state for the reaction of **2** has a slightly higher electric field strength than that of **1**, but still has a relatively low field strength. Thus, a spectrum of different affinity sequences may be observed depending on the electric field strength of the anion. The transition state for the reaction of phosphinate **3** with ethoxide corresponds to the high field strength end of the spectrum, while the transition states for sulfonates **1** and **2** correspond to the low to intermediate field strength end of the spectrum (Figure 6).

The present work therefore presents further evidence supporting the hypothesis that electric field strength of the transition state determines the trend in its metal-ion association constants. Two sulfonate esters, **1** and **2**, both react to give charge-delocalized transition states having low electric field strength; consequently, both interact with solvated metal ions and give similar trends in association constants. In contrast, the phosphinate ester **3** reacts via a charge-localized transition state having a high electric field strength and interacts with bare metal ions, resulting in a trend in association constants that differs from those of **1** and **2**. This, in turn, leads to a different ordering of reactivity of alkali-metal ethoxides.

Conclusions

The results presented here allow a number of conclusions to be made regarding the role of alkali-metal ions in the nucleophilic displacement reaction of ethoxide with *p*-(trifluoromethyl)phenyl methanesulfonate. Kinetic data for the reaction of alkali-metal ethoxides with **1** reveal the order of reactivity, LiOEt < EtO^- < NaOEt < CsOEt < KOEt, which is identical with that of *p*-nitrophenyl benzenesulfonate (**2**).[1g] In both systems, Li^+ inhibits the reaction, while Na^+, K^+, and Cs^+ accelerate the reaction.

The catalytic and inhibitory effects of alkali-metal ions in the reaction of **1** are discussed in terms of ground-state (δG_{ip}) and transition-state (δG_{ts}) stabilization. These effects can be summarized in the size of $\Delta G_{cat.}$, the difference in transition-state and ground-state stabilization. The values of $\Delta G_{cat.}$ are −2.2, −1.7, −1.5, and +1.7 kJmol^{-1} for K^+, Cs^+, Na^+, and Li^+, respectively, indicating that K^+ is the best catalyst, Cs^+ and Na^+ are less effective catalysts, and Li^+ is an inhibitor. These results are qualitatively similar to the results for **2**.

Comparison of alkali-metal ion affinity sequences for the transition states in reactions of ethoxide ion with esters **1–3** reveals significant differences. The observed affinity sequences are consistent with interactions of transition state for **1** with solvated metal ions and of the transition state for **3** with bare metal ions. Such a result is reasonable since interactions with solvated metal ions are expected for transition states with low electric field strengths, i.e., those in which charge is delocalized over a number of atoms, while interactions with bare metal ions are expected for transition states with high electric field strengths and localized charge. Charge is delocalized over two atoms in the transition state of **1** but is localized on one atom in the transition state of **3**. These results provide further evidence supporting our previous arguments regarding the interaction of charge-delocalized transition states with solvated metal ions.

Experimental Section

Materials. The general procedure of Crossland and Servis was followed for the synthesis of the *p*-(trifluoromethyl)phenyl methanesulfonate.[16] *p*-(Trifluoromethyl)phenol (0.02 mol) was dissolved in dry ether (100 mL), and redistilled Et_3N (4.2 mL, 0.03 mol) was added. Methanesulfonyl chloride (1.8 mL, 0.022 mol) was added dropwise from a syringe with stirring. The reaction mixture was stirred under nitrogen for approximately 1 h, and completeness of the reaction was checked by TLC. The reaction mix was transferred to a separatory funnel and extracted with distilled water (3 × 30 mL), 10% aqueous HCl solution (3 × 30 mL), saturated aqueous $NaHCO_3$ solution (3 × 30 mL), and saturated aqueous NaCl solution (30 mL). The organic solution was dried over anhydrous Na_2SO_4, filtered, concentrated under reduced pressure, and the crude product was repeatedly recrystallized from ethanol to a constant melting point (mp 43–44 °C). The purified ester gave excellent ^1H and ^{13}C NMR spectra and IR spectra, as well as elemental analysis.

Anhydrous ethanol, 18-crown-6, cryptands, and alkali-metal ethoxides were prepared and/or purified as described previously.[1g]

Kinetic Methods. Reaction rates were measured by following UV–vis absorbance changes due to the release of aryl oxide ion using a Perkin-Elmer Lambda 5 spectrophotometer. All reactions were carried out under pseudo-first-order conditions with the base in excess. The base concentration was at least 10 times greater than the substrate concentration and usually more than 20 times greater. The solutions were equilibrated to 25.0 °C in the thermostated cell block of the spectrophotometer and maintained at 25.0 ± 0.1 °C during reaction.

Rate constants were calculated from at least 30 absorbance readings spanning 3 half-lives. An infinity absorbance reading was taken after at least 10 half-lives. Rate constants were calculated as the slope of a plot of ln $(A_\infty - A_t)$ vs time. It is estimated that the error in any particular measured rate constant is not greater than ca. ± 3%.

Acknowledgment. This research was supported by the Natural Sciences and Engineering Research Council of Canada (NSERC). The awards to M.J.P. of a Postgraduate Scholarship by NSERC and a Graduate Award by Queen's University are gratefully acknowledged.

Registry No. **1**, 37903-93-8; **2**, 3313-84-6; **3**, 10259-20-8; LiOEt, 2388-07-0; NaOEt, 141-52-6; KOEt, 917-58-8; CsOEt, 18008-43-0; Li^+, 17341-24-1; Na^+, 17341-25-2; K^+, 24203-36-9; Cs^+, 18459-37-5.

(16) Crossland, R. K.; Servis, K. L. *J. Org. Chem.* **1970**, *35*, 3195.